Poly(2-allylamidopropyl-2-oxazoline) based hydrogels: from accelerated gelation kinetics to *in vivo* compatibility in a murine sub-dermal implant model

Tim R. Dargaville[1,2,3]*, Damien G. Harkin[3,4], Jong-Ryul Park[1,2,3], Amanda Cavalcanti[1,2,3], Eleonore C.L. Bolle[1,2,3], Flavia Medeiros Savi[3], Brooke L. Farrugia,[5] Bryn Monnery[6], Yann Bernhard[6], Joachim F. R. Van Guyse[6], Annelore Podevyn[6], Richard Hoogenboom[6]*

A/Prof Tim R. Dargaville, Prof Damien G. Harkin, Jong-Ryul Park, Dr Amanda Cavalcanti, Dr Eleonore Bolle

1. Centre for Materials Science, Queensland University of Technology, 2 George Street, Brisbane, QLD 4000, Australia.

2. School of Chemistry and Physics, Queensland University of Technology, 2 George Street, Brisbane, QLD 4000, Australia.

3. Institute of Health and Biomedical Innovation, Science and Engineering Faculty, Queensland University of Technology, Queensland 4001, Australia

4. School of Biomedical Sciences, Queensland University of Technology, 2 George Street, Brisbane, QLD, 4000, Australia.

Dr Brooke L. Farrugia

5. Department of Biomedical Engineering, The University of Melbourne, Victoria 3010, Australia

Dr. Joachim F. R. Van Guyse†, Annelore Podevyn, Dr. Bryn Monnery‡, Dr. Yann Bernhard, Prof Richard Hoogenboom

6. Supramolecular Chemistry group, Centre of Macromolecular Chemistry (CMaC), Department of Organic and Macromolecular Chemistry, Ghent University, Krijgslaan 281 S4, B-9000 Ghent, Belgium

† Current address: Innovation Centre for Nanomedicine, Kawasaki Institute for Industrial Promotion, 3-25-14 Tono-machi, Kawasaki-ku, Kawasaki City, Kanagawa Prefecture, Japan

‡ Current address: Department of Organic and Bio-Polymer Chemistry, Hasselt University, Building D, Agoralaan, Diepenbeek, B-3590 Belgium

_____

TOC image

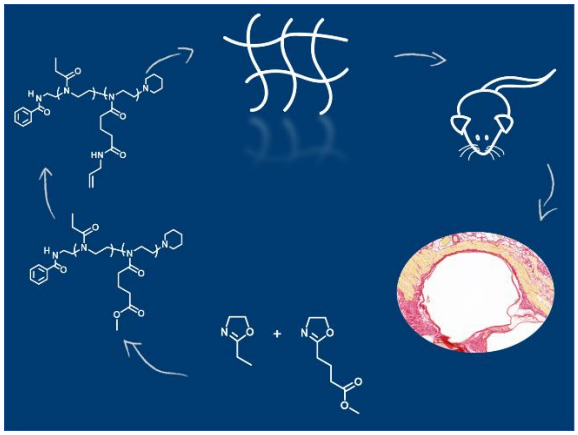

Highlights

- facile synthesis of a novel poly(2-oxazoline) containing allyl-amidopropyl side-chains

- photo-hydrogelation for rapid crosslinking

- foreign body response similar to the gold standard, PEG, in a murine model

Keywords: foreign body response, hydrogel, poly(2-oxazoline), thiol-ene

Abstract

A rapid photo-curing system based on poly(2-ethyl-2-oxazoline-*co*-2-allylamidopropyl-2-oxazoline) and its *in vivo* compatibility are presented. The base polymer was synthesized from the copolymerization of 2-ethyl-2-oxazoline (EtOx) and the methyl-ester containing 2-methoxycarboxypropyl-2-oxazoline (C_3MestOx) followed by facile amidation to yield a highly water soluble macromer. We showed that spherical hydrogels can be obtained by a simple water in oil gelation method using thiol-ene coupling and investigated the *in vivo* biocompatibility of these hydrogel spheres in a 28 day murine sub-dermal model. For comparison, hydrogel spheres prepared from poly(ethylene glycol) were also implanted. Both materials displayed mild, yet typical foreign body responses with little signs of fibrosis. This is the first report on the foreign body response of a poly(2-oxazoline) hydrogel, which paves the way for future investigations into how this highly tailorable class of materials can be used for implantable hydrogel devices.

Introduction

The continued application of synthetic hydrogels in a broad range of biomedical applications, ranging from drug delivery[1] to tissue engineering,[2] has sustained ongoing interest in the discovery of new polymers with the required properties. These requirements include cytocompatibility, minimal foreign body response (FBR), high yielding, rapid crosslinking under mild conditions, few or no side reactions or release of small molecules, simple formulation, and availability of cheap and readily available or easily synthesized starting materials. Taking these properties into consideration, our previous work has been aimed at developing new hydrogels based on poly(2-alkyl-2-oxazoline)s (PAOx).[3,4] The rationale behind using PAOx over other non-ionic, hydrophilic materials is their rich chemistry, relatively straight-forward and controlled synthesis, and their biocompatibility (at least for non-crosslinked PAOx).[5] A comprehensive discussion highlighting the attractiveness of PAOx as a base material for hydrogels has been recently published.[6]

The methods for preparing hydrogels from PAOx are based on network formation during the cationic ring opening polymerization (CROP) of 2-oxazolines by using bis-functional monomers followed by solvent exchange to water,[7,8] or the synthesis of functional polymers, i.e. macromers, that are subsequently crosslinked chemically,[9,10] enzymatically,[11,12] or by using an external stimulus.[3,4,13,14] The first of these methods is useful for making gels rapidly and inexpensively, but since organic solvents are needed for the *in situ* polymerization and crosslinking of 2-oxazolines, it is not an approach that can be used to encapsulate biological macromolecules or cells. Alternatively, synthesizing functional PAOx followed by crosslinking in an aqueous environment can overcome these challenges. Even though the range of functional PAOxs that are available for this approach is still limited, it is continuously expanding.[15]

Despite the growing interest in PAOx hydrogels for biomedical applications, there is a scarcity of *in vivo* data. Soluble and nanoparticle formulations of PAOx are known to be well-tolerated in both animals[6] and data from a relatively small and preliminary human clinical trial suggests the polymer is safe and well-tolerated.[16,17] Yet for PAOx hydrogels, the only reports on *in vivo* behavior are based on a PAOx-collagen conjugate for hemostatic wound-dressing in a porcine model,[18] a thermo-gelling poly(2-ethyl-2-oxazoline) copolymer implanted in rats for up to 12 hours,[19] and mesenchymal stromal cell-loaded PAOx hydrogels in a murine infarction model.[20] Aside from these examples, no data has been published on the longer term *in vivo* compatibility of PAOx hydrogels. Furthermore, as the parameter space of PAOx materials is vast, each composition much be considered and evaluated on a case-by-case basis.[21]

The *in vivo* compatibility of implanted hydrogels can be assessed by viewing the foreign body response (FBR) to these materials. This immune-mediated response is an almost unavoidable event following implantation of a hydrogel into the body. A FBR can lead to fibrotic encapsulation and reduced function, rejection or failure of the hydrogel. The severity of the FBR, however, depends on the material and can range from acute to negligible.[22] Rational design parameters to control the FBR of materials are not predictable from first principles/theory and, therefore, *in vivo* experimentation of any new materials is necessary to properly evaluate the FBR.[23-25]

Over the past several years, we have developed hydrophilic PAOx copolymers with alkene-terminated alkyl side-chains using 2-undecenyl-2-oxazoline (DecenOx) or 2-butenyl-2-oxazoline (ButenOx) copolymerized with 2-methyl-2-oxazoline (MeOx) or 2-ethyl-2-oxazoline (EtOx).[3,4,14] These polymers can be crosslinked by a range of multi-thiol containing molecules *via* thiol-ene coupling. A disadvantage of these materials is that the alkenyl side-chains are rather hydrophobic and in order to maintain water solubility, copolymerization with high feed ratios of the hydrophilic MeOx is necessary. Furthermore, it was previously found that incorporation of DecenOx leads to faster photocuring kinetics during hydro-gelation by local aggregation of the alkene side-chains, which is accompanied by partial homocoupling at the expense of the thiol-ene reaction.[3] This homocoupling side-reaction compromises the control over the network structure as well as biodegradability when using degradable crosslinkers.

In this study, we utilized a previously reported monomer, 2-methoxycarboxypropyl-2-oxazoline (C_3MestOx) (Scheme 1A),[9,26-30] and copolymerized it with EtOx by living cationic ring-opening polymerization, followed by amidation of the methyl ester of the C_3MestOx units with allylamine to obtain a highly water soluble polymer containing side-chain allyl-amidopropyl groups suitable for crosslinking (Scheme 1B,C). The kinetics of the photo-hydro-gelation reaction and the cytotoxicity of the precursors are reported together with the first *in vivo* evaluation of the FBR to the PAOx hydrogel, bench-marked against a polyethylene glycol (PEG) hydrogel, to provide crucial animal safety data and thereby laying the foundations for further biomaterial applications.

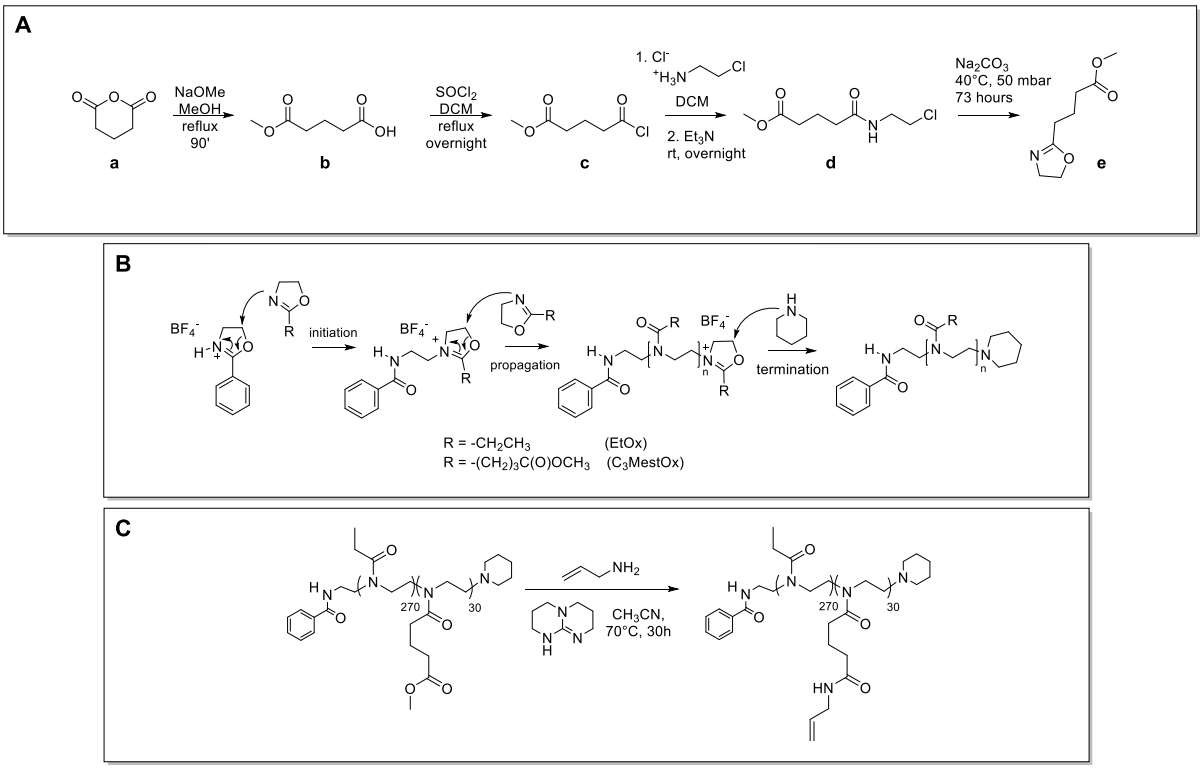

Scheme 1: A) Modified Wenker method: general synthesis route for the preparation of C_3MestOx starting from glutaric anhydride; B) Cationic ring-opening polymerization (CROP) mechanism of EtOx and C_3MestOx with an oxazolinium salt (2-phenyl-2-oxazolinium tetrafluoroborate (HPhOx-BF_4)) as initiator and piperidine as terminator; C) Allyl-amidation of the methyl ester side-chains of P($EtOx_{270}$-$C_3MestOx_{30}$) using 6 equivalents of allylamine relative to ester groups and 1,5,7-triazabicyclo[4.4.0]dec-5-ene (TBD) as catalyst in CH_3CN.

Materials and Methods

All materials for the synthesis of the polymers were obtained from Merck unless stated otherwise. Glutaric anhydride was obtained from TCI. Polymer Chemistry Innovations kindly donated the 2-ethyl-2-oxazoline which was distilled over BaO (90%, Acros) and ninhydrin prior to use and stored in a glovebox under inert and dry conditions. Irgacure 2959 (I2959; 2-hydroxy-4'-(2-hydroxyethoxy)-2-methylpropiophenone) was a gift from BASF. Synthesis of 2-phenyl-2-oxazolinium tetrafluoroborate (HPhOx-BF_4)[31] and 2-methoxycarboxypropyl-2-oxazoline (C_3MestOx)[30] was conducted according to

the previously published procedures. Piperidine was distilled over CaH_2 prior to use. Dry solvents were obtained from a solvent purification system from J.C. Meyer, with aluminium oxide drying columns and a nitrogen flow. Deuterated solvent for ^{1}H NMR spectroscopy, i.e. chloroform-*d* ($CDCl_3$, ≥99.8% D, water <0.01%), was purchased from Euriso-top. Irgacure 2959 (2-hydroxy-4'-(2-hydroxyethoxy)-2-methylpropiophenone) was a gift from BASF and was used as received. Two PEG precursors (4-arm PEG-SH 5 kDa and 4-arm PEG-vinyl sulfone 20kDa) were obtained from JenKem Technology. Poly(dimethylsiloxane) (viscosity 40 cSt) was obtained from Alfa Aesar.

Copolymerization of C_3MestOx and EtOx

Copolymerization of 2-ethyl-2-oxazoline (EtOx) with 10 mol% C_3MestOx was performed using a modified literature method.[31,32] All glassware was cleaned and dried in a 200 °C oven before being silanized with chlorotrimethylsilane (TMS-Cl) to render the glass surface hydrophobic and prevent ordered water forming. Next, 2-phenyl-2-oxazolinium tetrafluoroborate salt (60.6 mg, 0.258 mmol, 0.003 equiv) was added to the flask as initiator and melted under active vacuum (1.6×10^{-1} mbar). The silanized flask was transferred under inert and dry atmosphere to a glovebox, where the monomers, EtOx (7.85 mL, 77.76 mmol, 0.9 equiv) and C_3MestOx (1.29 mL, 8.64 mmol, 0.1 equiv), and the dry solvent (acetonitrile, 8.87 mL) were added. The mixture was stirred vigorously and a t = 0 sample was taken as a reference to follow the conversion *via* gas chromatography (GC) and ^{1}H NMR spectroscopy. To obtain a P(EtOx-C_3MestOx) copolymer with a target degree of polymerization (DP) of 300 at 91.5% conversion, the reaction mixture was immersed in an oil bath at 60 °C for 60 hours. After the reaction, 51 µL of piperidine was added at 0 °C and the resulting mixture was stirred overnight. Purification was performed by precipitation of the copolymer in ice-cold diethyl ether followed by dialysis (MWCO = 3.5 kDa) and subsequent lyophilization to obtain the P(EtOx-C_3MestOx) as a white, fluffy powder (M_n = 17 kg/mol, Đ = 1.35). Full characterization was done using gas chromatography (to check monomer conversion at the end of the polymerization), size-exclusion chromatography (SEC) and ^{1}H NMR spectroscopy.

Post-polymerization modification of P(EtOx$_{270}$-stat-C_3MestOx$_{30}$) by amidation with allylamine

The P(EtOx-C_3MestOx) copolymer containing 10 mol% (30 units) of methyl ester sidechains was functionalized in a post-polymerization amidation reaction with allylamine. P(EtOx-C_3MestOx) copolymer (2 g, 0.0719 mmol), containing 2.156 mmol of functional methyl ester groups (1 equiv), was dissolved in 15.4 mL of acetonitrile with 1,5,7-triazabicyclo[4.4.0]dec-5-ene (TBD, 150 mg, 1.078 mmol, 0.5 equiv) as a catalyst. Subsequently, allylamine (0.97 mL, 12.9 mmol, 6 equiv) was added and the mixture was reacted at 70 °C for 30 hours to full conversion. The purification was performed by precipitation in ice-cold diethyl ether followed by dialysis (MWCO = 1 kDa) and subsequent lyophilization. The polymer was obtained as a white fluffy powder. Full modification of the methyl ester side-chains to allylamidopropyl side-chains leading to *P(EtOx-stat-2-allylamidopropyl-2-oxazoline)* (PEAOx) was confirmed using ^{1}H NMR spectroscopy and SEC (Mn = 23.7 kg/mol, Đ = 1.22).

Photo-rheology

Gelation kinetics were studied by performing small strain oscillatory shear experiments on an Anton Paar MCR302 Rheometer with 10 mm parallel plate-plate geometry at 30 °C. Samples were irradiated using an Omnicure Series 2000 ultraviolet light source with 365 nm filter and a fibre optic probe fitted under the quartz bottom plate of the rheometer. An example of how a polymer sample was prepared is as follows: to make a 10% PEAOx hydrogel with 1:1 thiol-to-ene stoichiometry, 75 µL of a 12% wt/vol solution of PEAOx in water was mixed with 6.4 µL of a 10% dithiothreitol solution, 4.5 µL of 2% I2959 solution, and 4.1µL distilled water to make a total of 90 µL. Aliquots of this solution (28 µL) were pipetted onto the quartz plate and the test started with the UV source turned on after either 30 or 60 s of collecting baseline data. After irradiation the samples were recovered, washed in water, freeze dried and weighed to determine swelling ratios.

Cell viability studies

Human foetal fibroblasts were obtained from the Prince of Wales Hospital (Human Research Ethics Committee project 02247) and were seeded at 50,000 cells per sample in Dulbecco's Modified Eagle's Medium (DMEM) supplemented with 10% foetal bovine serum (FBS), and L-glutamine (2mM). After

overnight incubation at 37 °C in 5% CO_2, the culture medium was changed to fresh DMEM with the FBS being replaced with 0.1% bovine serum albumin (BSA). H_2O_2 (200 mM; positive control for toxicity) or soluble PEAOx (0.25-2 mg/mL) were subsequently added to cells in this medium and incubated for 6 hours. The medium was then discarded and cells were washed in PBS before addition of CellTiter 96® AQueous MTS solution (Promega, Cat# G3582) diluted 1:10 with DMEM. Absorbance at 490 nm was measured after 1 hour incubation. Data is presented as the mean with s.e.m expressed as the percentage change in absorbance from the control after background correction of MTS solution alone.

Hydrogel sphere generation

A stock solution containing PEAOx (60 mg, 1.684 mmol), dithiothreitol (3.9 mg, 25.2 mmol, 0.5 eq. relative to the alkene of the PEAOx) was prepared in 510 µL of PBS (pH 7.3), and 30 µL 2% w/v I2959 in water was added just prior to the solution being loaded into a syringe. The polymer solution was then added dropwise through a 29G needle into 10 mL of poly(dimethylsiloxane) (PDMS) oil stirred at 400 rpm with a 1.5 cm long magnetic stirrer bar in a 25 mL round bottom flask. The suspension was then irradiated with UV light (Omnicure S2000, 365 nm) for 10 min with continued stirring. The resulting hydrogels spheres were washed with 200 mL of dichloromethane and filtered five times, then washed with acetone (5×) and ethanol (5×). Absence of residual PDMS was confirmed by ^{1}H NMR spectroscopy by soaking the spheres in $CDCl_3$ then acquiring spectra on the washing solution. The hydrogel spheres were finally washed with ultrapure ethanol (1×) and sterile PBS (5×) under aseptic conditions in a laminar hood prior to implantation into mice. Control PEG hydrogel spheres were synthesized in a similar manner. A solution containing 5 kDa 4-arm PEG-SH (15 mg; 3 mmol) and 20 kDa 4-arm PEG-vinyl sulfone (45 mg; 2.3 mmol) was prepared in 540 µL of PBS (pH 7.3) and pre-cured for 10 min before adding dropwise into 10 mL of PDMS oil using identical conditions as for the PEAOx spheres but without UV irradiation. After adding the solution dropwise, the reaction was continued for 30 min then washed and prepared for implantation using the same protocol as above.

Murine model for in vivo determination of foreign body response

The experiments involving animals were undertaken following the Australian Code for the Care and Use of Animals for Scientific Purposes (8th Edition: 2013)[33] and the Queensland University of Technology Code of Conduct for Research and were approved by the University Animal Ethics Committee. A total of six 8-week-old male C57BL/6 mice (body weights, 23±1 g) were purchased from Animal Resources Centre (WA, Australia). Animals received water *ad libitum* and were fed with an irradiated rodent diet. Mice were housed in specific pathogen-free conditions (filtered rack, Tecniplast) under 12 hour light/dark cycles at the Medical Engineering Research Facility (QUT, Australia). Mice were anesthetized with isoflurane (Laser Animal Health) and subcutaneous administration of Meloxicam (1 mg/kg) and buprenorphine (0.05 mg/kg) were used as pre-emptive analgesia. In ventral recumbency, the upper and lower areas of the dorsum were clipped and painted with 10% povidone-iodine (Betadine) followed by four longitudinal incisions (approximately 3 mm) and subcutaneous pockets were formed *via* blunt dissection. Four hydrogel samples - two sets of 10× PAOx spheres and two sets of 10× PEG spheres were placed into the pockets using forceps. The wounds were closed with sutures. Tramadol (25 mg/L) were offered in the drinking water for five days after surgery as post-operative analgesia. Mice were monitored daily for 28 days when the euthanasia was performed with CO_2 asphyxiation in an appropriate chamber, and the hydrogels samples were collected and processed for histological analysis to examine the *in vivo* FBR.

Histology

Tissue explants were immersed in 4% paraformaldehyde in PBS overnight, washed in 70% v/v ethanol, then were dehydrated through a series of graded ethanol baths to displace the water, and infiltrated with wax using an Excelsior™ AS Tissue Processor (Thermo Fisher Scientific Inc.). The infiltrated tissues were then embedded into wax blocks using the Shandon Paraffin Embedding Station (Thermo Fisher Scientific Inc.). Each embedded tissue sample was cut into 5 µm sections and stained for analysis of general morphology with hematoxylin and eosin (H&E) using a high throughput autostainer (Leica ST5010 Autostainer XL). Additional sections were stained for examination of potential differences in fibrotic response using Masson's Trichrome, Picro-Sirius Red and immunostaining for alpha-smooth muscle actin (α-SMA). These staining procedures were performed at the Histology Facilities at the

Institute of Health and Biomedical Innovation and the Translation Research Institute (both QUT, Australia). Two experienced histologists independent to the design and experimental work (co-authors DGH and BLF) gave blind assessments of the sections.

Instrumentation

Samples were measured with GC to determine the monomer conversion based on the ratio of the integrals from the monomer and the reaction solvent. GC was performed on an Agilent Technologies 7890A system equipped with a VWR Carrier-160 hydrogen generator and an Agilent Technologies HP-5 column of 30 m length and 0.320 mm diameter. A flame ionization detector was used and the inlet was set to 250 °C with a split injection of ratio 25:1. Hydrogen was used as carrier gas at a flow rate of 2 mL/min. The oven temperature was increased with 20 °C min^{-1} from 50 °C to 120 °C, followed by a heating ramp of 50 °C min^{-1} from 120 °C to 300 °C.

SEC was performed on an Agilent 1260-series HPLC system equipped with a 1260 online degasser, a 1260 ISO-pump, a 1260 automatic liquid sampler (ALS), a thermostat-controlled column compartment (TCC) at 50 °C equipped with two PLgel 5 µm mixed-D columns and a precolumn in series, a 1260 diode array detector and a 1260 refractive index detector. The eluent was *N*,*N*-dimethylacetamide (DMAc) containing 50 mM of LiCl at a flow rate of 0.5 mL min^{-1}. The SEC elugrams were analysed using the Agilent Chemstation software with the GPC add on. Molar mass values and Đ values were calculated against PMMA standards from PSS.

Lyophilisation was performed on a Martin Christ freeze-dryer, model Alpha 2-4 LSC plus.

Monomers were stored and polymerisation mixtures were prepared in a VIGOR Sci-Lab SG 1200/750 Glovebox System with obtained purity levels below 1 ppm, both for water and oxygen content.

NMR spectra were recorded on a Bruker Avance 400 MHz spectrometer at room temperature.

Results and Discussion

Synthesis of 2-methoxycarboxyethyl-2-oxazoline, copolymerization and amidation

The C_3MestOx monomer was synthesized in four steps using previously published methods (Scheme 1A)[30] and the structure of the distilled product was verified by ^{1}H NMR spectroscopy (Figure S1). The subsequent copolymerization with commercially available 2-ethyl-2-oxazoline (EtOx) in a 9:1 molar ratio (9:1 EtOx:C_3MestOx) was achieved by conventional heating at 60 °C with 2-phenyl-2-oxazolinium tetrafluoroborate salt as an initiator and a target DP of 300 (Scheme 1B). Size exclusion chromatography (SEC) of the copolymer (Figure 2) revealed a dispersity (Đ) of 1.35 including a slight high molar mass shoulder as a result of chain-coupling side reactions known to occur in 2-oxazoline polymerizations.[31] Some insight into the structure of the copolymer can be obtained from the propagation rate constants of the two monomers. In a previous kinetics study of the copolymerization of EtOx and C_3MestOx[28] slightly faster consumption of the EtOx monomer was reported resulting in a polymer with a gradual gradient resulting from a larger proportion of C_3MestOx being copolymerized at higher conversion, but as discussed later, any slight gradient in monomer incorporation did not impact the ability to form high yielding hydrogels.

To introduce the allyl groups for thiol-ene crosslinking to the side-chains of the copolymer a simple amidation reaction with an excess of allylamine in presence of TBD as catalyst was performed (Scheme 1C).[29,34] SEC of the allylamidopropyl functionalized product, denoted PEAOx, showed an increase in molar mass while ^{1}H NMR spectroscopy confirmed the full consumption of the methyl-ester and the incorporation of the allyl groups and the methylene next to the secondary amide (Figure 2).

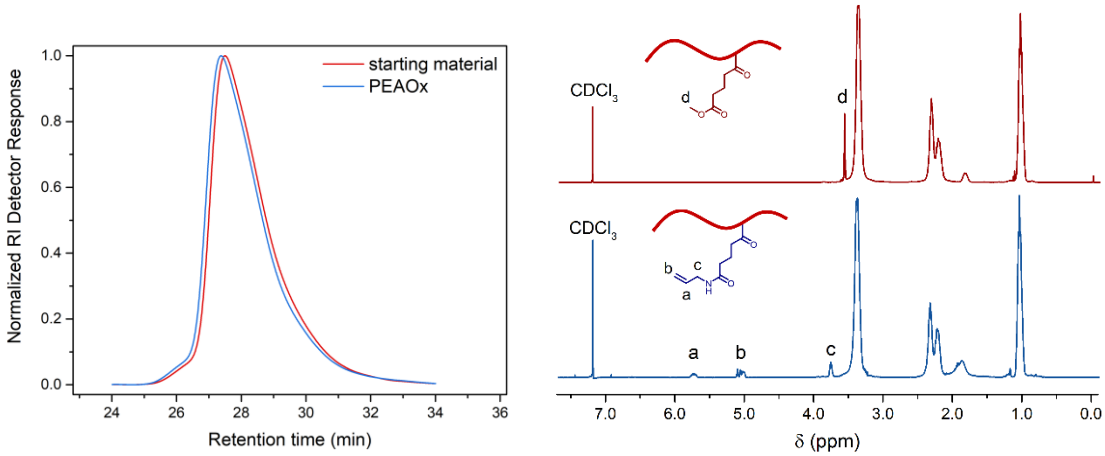

Figure 2: RI elugram of size exclusion chromatography (**left**) and ^{1}H NMR spectroscopy results (**right**) of the allylamine amidation of P(EtOx$_{270}$-C$_3$MestOx$_{30}$).

Hydro-gelation via thiol-ene coupling

The hydro-gelation of PEAOx *via* thiol-ene photo-crosslinking with dithiothreitol as the crosslinker and Irgacure 2959 as the photoinitiator was investigated in real-time by photorheology using a range of mole fractions (χ) of thiol-to-alkene. The gelation kinetics showed rapid crosslinking; on the order of 15 sec after illumination of the UV light (Figure 3 left) with a maximum in the final modulus around a χ of 0.5 (Figure 3 right), although the reaction is relatively insensitive to dithiothreitol in the range χ = 0.25 to 1. When $\chi > 1$ the G'_{max} was much lower presumably due to the larger excess of thiol groups leading to mono-coupling of the dithiols, thereby reducing the amount of network yielding thiol-ene reactions. Interestingly, when no thiol was used, gelation was absent. This is contrary to our previous findings for the hydro-gelation of a poly(2-methyl-2-oxazoline-*co*-2-decenyl-2-oxazoline) (PMeOx-DecenOx) copolymer where homocoupling of vinyl groups resulted in gelation even without the dithiol present.[3] This was ascribed to the aggregation of the hydrophobic decenyl side-chains leading to high local alkene concentration that facilitates the homocoupling. Similar aggregation should be absent in PEAOx due to the more polar allyl-amidOx units thereby avoiding homocoupling. Previously, we hypothesized that this aggregation of DecenOx side-chains led to faster hydro-gelation of DecenOx copolymers compared to the ButenOx copolymers that do not aggregate. Surprisingly, the photogelation kinetics of PEAOx was found to be even faster when directly compared to the PMeOx-DecenOx

copolymer (Figure S2), suggesting higher efficiency of the thiol-ene reaction even without aggregation and higher local concentration of the double bonds.

It may be speculated that the allyl groups in PEAOx are more accessible for crosslinking with the hydrophilic DTT dithiol due to the presence of the long, hydrophilic amidopropyl spacer and that it is not related to potentially, higher reactivity of the allyl-groups. To test this hypothesis, two other non-aggregating hydrophilic polymers were prepared with allyl and pentenyl side-chains, namely copolymers of hydroxyethylacrylamide with allylacrylamide and pentenylacrylamide (each with 3 or 10 mol% comonomer incorporation) (structures shown in Figure 4). These copolymers were prepared through amidation of poly(methyl acrylate) with a mixture of 2-aminoethanol and allylamine or pentenylamine following our recently reported protocol.[35] Photorheology for the curing of these polymers revealed faster hydro-gelation for the pentenylacrylamide compared to the allylacrylamide containing copolymers (Figure S3). Although comparing two different polymer systems does not allow for absolute comparisons due to other factors, such as polymer conformation, we can tentatively suggest that the observed faster hydro-gelation of PEAOx is related to higher exposure of the allyl groups to the solvent, resulting from the longer, hydrophilic spacer between the backbone and the allyl-groups and not simply higher reactivity of the allyl groups (details for the synthesis and photocuring of these polyacrylamides are provided in the supporting information).

Aside from the improved gelation kinetics, another advantage stemming from the use of the C_3MestOx monomer and its subsequent allylamido product, is that the copolymer with EtOx is water soluble while, in contrast, the previously reported DecenOx copolymers with EtOx were water insoluble and had to be cured in ethanol.[14,36] Thus, DecenOx is limited to being copolymerized with very hydrophilic monomers (e.g. MeOx) when a water soluble polymer is desired.[3] Other advantages of PEAOx compared to the DecenOx copolymers are its rapid dissolution in water (within seconds) and its lack of surfactant-like properties, facilitating the manipulation of the polymer solution without generating bubbles, leading to defect-free hydrogels.

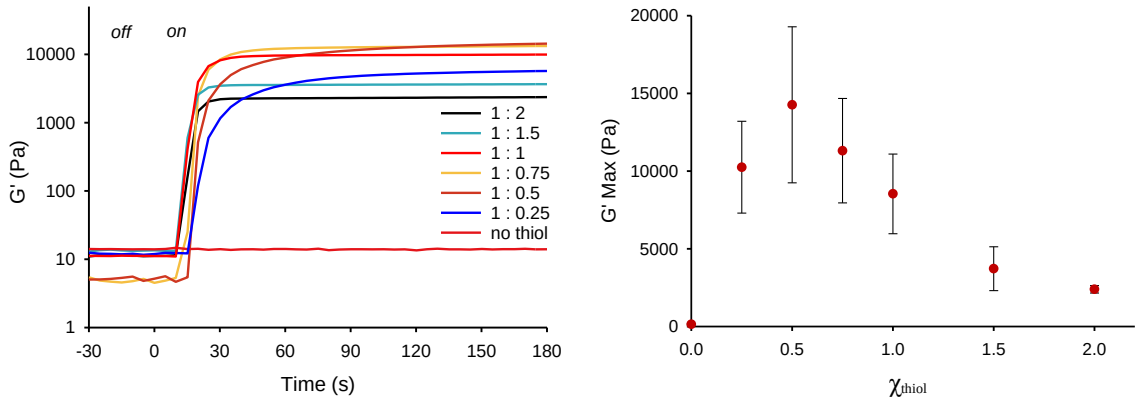

Figure 3: (Left) Representative curves of storage moduli (G′) of 10% PEAOx solutions with different thiol:ene ratios before and during irradiation with 365 nm UV light, I2959 concentration 0.1% wt/v, (right) dependence of thiol-ene ratio on maximum storage moduli (G'_{max}).

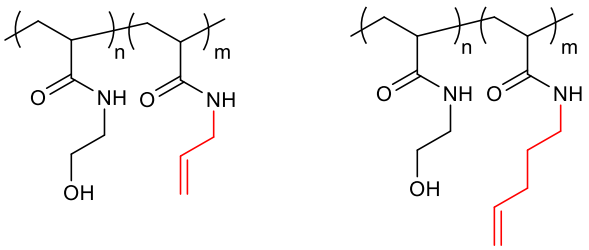

Figure 4: Structures of poly(hydroxyethylacrylamide-*co*-allylacrylamide) (left) and poly(hydroxyethylacrylamide-*co*-pentenylacrylamide) (right). The allyl and pentenyl groups are highlighted in red.

Cell viability and foreign body response of PEAOx

To test the cytotoxicity of PEAOx, human foetal fibroblasts were exposed to polymer solutions with concentrations of up to 2 mg/mL in a cell viability study. According to the standard MTS metabolic assay (Figure S4), the solutions were non-toxic at these concentrations. This result is not surprising considering the structural similarities to PEtOx which is known to be non-toxic in rats after multiple doses of 50 mg/kg of a similar molar mass polymer as used here.[37]

To evaluate the FBR response of crosslinked PEAOx hydrogels, the polymer was formulated into spherical hydrogel geometries. PAOx hydrogel spheres have been prepared previously using emulsion[38] and microfluidic methods[39] with PMeOx-diacrylate. However, for this study, we chose to prepare hydrogel spheres by a simple method of dropping an aqueous solution of PEAOx, dithiothreitol and I2959 into stirred poly(dimethylsiloxane) oil (PDMS) followed by irradiating with UV light until stable, crosslinked hydrogel spheres were formed. As a control, PEG-VS/PEG-SH hydrogels were prepared in a similar manner but without the need for UV light as the vinyl-sulfone thiol reaction occurs *via* spontaneous Michael-type addition.[40,41] This system was chosen as it uses facile crosslinking chemistry, does not contain any hydrolytically sensitive ester groups and the hydrogel pre-cursors are commercially available. All spheres were exhaustively washed with ethanol until no PDMS was detectable by ^{1}H NMR spectroscopy.

The size distributions of the spheres were measured using light microscopy and ranged from 0.75–1.75 mm for PEAOx spheres and 1.25–2.35 mm for PEG spheres (Figure S5). The average diameters were 1.3 mm and 1.9 mm for the PEAOx and PEG spheres, respectively. Although the conditions used to prepare the two types of spheres was similar, the variability in size distributions is probably due to the differences in hydrophilicity between PEAOx and PEG – PEAOx consists of mostly EtOx units which are known to be slightly less hydrophilic than PEG.[37] Furthermore, the number of crosslinking points, polymer architecture, the molar mass between crosslinks, and the solution viscosity all influence the sphere size. The equilibrium swelling ratio of PEAOx spheres was 10.0 ± 0.8, while for PEG spheres it was 17.0 ± 0.9 (n = 3 for both).

The murine *in vivo* model used to probe the FBR involved subcutaneous implantation of the hydrogel spheres into immuno-competent C57BL/6 mice followed by harvesting of the spheres and surrounding tissue from the euthanized mice after 28 days. This time point was chosen to allow for sufficient time for resolution of any acute inflammatory response due to the introduction of the implant and the establishment of granulation tissue and fibrous capsule formation.[42] The implantation of the spheres consisted of an incision of the skin and positioning of approximately ten spheres of PEAOx or PEG hydrogels into four subcutaneous pockets per animal – one group per shoulder and hip (Figure 5A-C).

After 28 days, the explanted hydrogel spheres and surrounding tissue (Figure 5D,E) were prepared for histological analysis. In all cases the hydrogels were recovered with no visual signs of degradation. This lack of degradation is in contrast to a study reported by Lynn *et al*., who observed that only 20% of 5 × 1 mm discs of PEG-acrylate[43] could be recovered from mice after 28 days. In their study, the presence of the cleavable ester in the acrylate group was hypothesized to be the source of initial degradation products leading to macrophage recruitment and subsequent complete degradation. The PEG used in our study, however, used vinyl sulfone-thiol coupling, hence no labile esters were present. Similarly, the PEAOx hydrogels used in the present study lack degradation sites and so would not be expected to hydrolytically degrade. For the polymer backbone, data from previous studies on PEtOx can be used as a guide – under simulated biological conditions,[44] and *in vivo* (based on unpublished stability data referenced by Moreadith *et al.*[16]) PEtOx is known to be stable. Although under simulated biological oxidative stress conditions, reactive oxygen species are postulated to degrade PEtOx.[45] The good integrity of the retrieved spheres implies the absence of substantial degradation over the time course of this experiment for the implantation site chosen. Note that the PEAOx hydrogels may be redesigned to become degradable by utilization of degradable dithiol crosslinkers, if desired for future work.

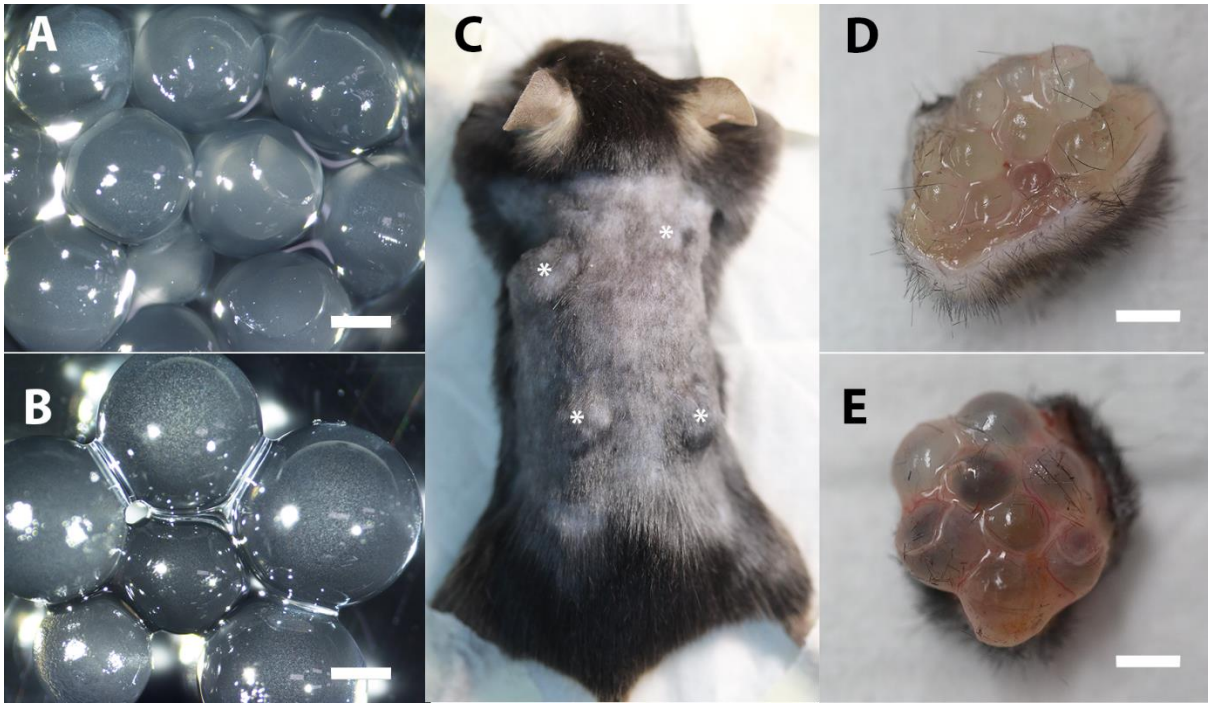

Figure 5: Murine *in vivo* foreign body response model: light microscopy images of PEAOx spheres (A) and PEG spheres (B) prior to implantation; implantation sites, four per animal, in the subcutaneous tissue indicated by * (C); photographs of tissue removed 28 days later displaying retention of integrity for PEAOx spheres (D) and PEG spheres (E), respectively. Scale bars: 1 mm for A,B; 2 mm for D,E.

The H&E, Picro-Sirius Red and trichrome stained sections of excised spheres and surrounding tissue demonstrated that the majority of PEG and PEAOx hydrogel spheres were successfully implanted within the stratum fibrosum layer (Figure 6). The hydrogel spheres displayed folding and often total displacement away from the host tissue, most likely due to processing of the explanted specimens for histology, as commonly observed for hydrogel implant experiments.[46] Nonetheless, the location of the spheres in the stained sections was clearly visible based on the circular imprints corresponding to the same diameters as the spheres (*ca.* 1-2 mm).

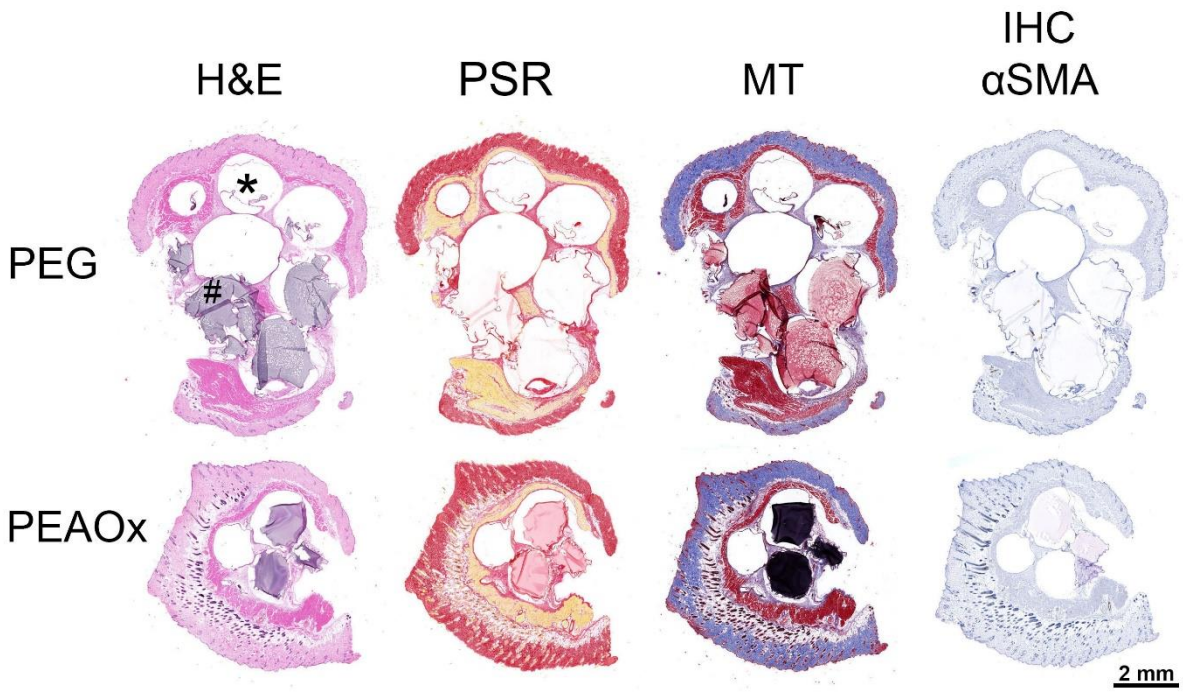

Figure 6: Low power views of representative serial histological sections of PEG (top row) and PEAOx (bottom row) hydrogel spheres implanted subcutaneously in mice stained for H&E, Picro-Sirius Red (PSR) and Masson's trichrome (MT) as well as immunohistochemical (IHC) staining for α-SMA. Hydrogel spheres were implanted for 28 days prior to tissue excision, fixation and processing. The majority of particles were successfully implanted within the stratum fibrosum beneath the panniculus muscle. The * denotes an example of the location of a hydrogel sphere lost during processing, while # donates an example of an intact hydrogel sphere.

Higher magnification images of the stained sections revealed a similar host response to both the PEG and PEAOx hydrogel spheres consisting of a thin capsule of presumptive monocytes immediately adjacent to the hydrogel microsphere surface (arrow in Figure 7). Neither the PEG nor the PEAOx stained sections showed any α-smooth muscle actin (α-SMA) in the regions adjacent to the hydrogel implants indicating the absence of myofibroblasts, which would be associated with a chronic inflammatory response. To further investigate the inflammatory response, sections were stained for nitric oxide synthase (iNOS; indicative of pro-inflammatory phenotype macrophages) and CD206 (indicative of reparative phenotype macrophages) (Figure S6) to reveal the presence of both types of macrophages within the adjacent connective tissue, but not immediately bordering the hydrogel implants, for both types of hydrogel materials. The presence of reparative macrophages in the connective tissue supports the observations from the α-SMA staining of an absence of chronic inflammation while also indicating a shift towards integration of the hydrogel spheres into the tissue.[47]

In response to both types of hydrogel spheres, the connective tissue immediately adjacent to each capsule consisted of vascularized connective tissue with the collagen fibers being more compressed towards the monocytic capsular layer highlighted in the trichrome stained sections and the Picro-Sirius Red stained sections under polarized light (Figure 8) to emphasize collagen fiber thickness and packing.[48] The alignment of collagen fibers adjacent to each implantation site was judged to be similar for each of the materials tested. However, the presence of the blood vessels (most evident in the trichrome, Picro-Sirius Red and α-SMA stains) in the connective tissue evidences the absence of the

dense avascular collagen capsule typically observed for materials eliciting a strong FBR, such as poly(2-hydroxyethyl methacrylate) hydrogels.[46] Only the occasional multi-nucleated giant cells (associated with a FBR) were observed in the tissue surrounding the PEG and PEAOx implants (Figure S7).

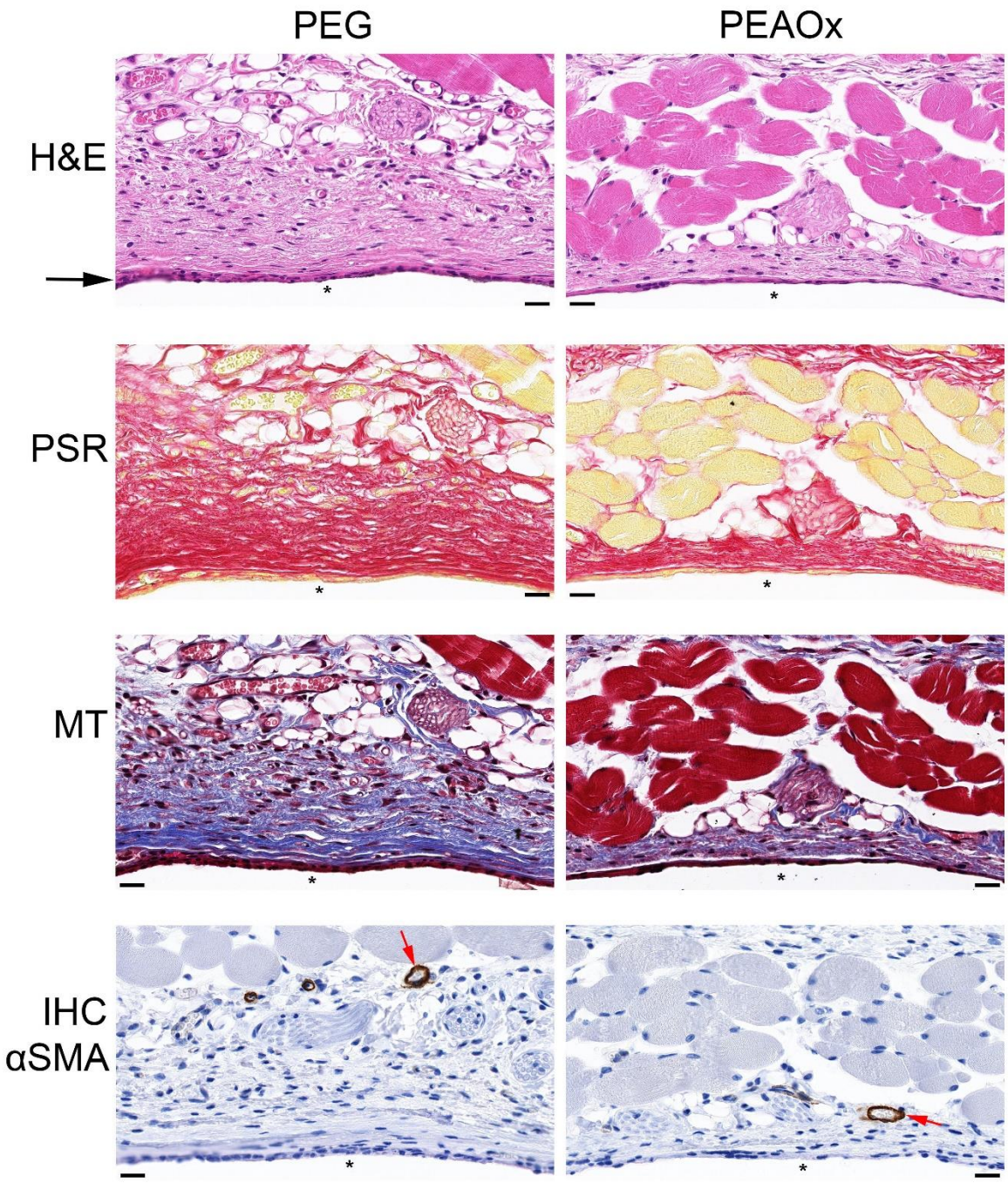

Figure 7: High power views of representative serial histological sections of PEG (left column) and PEAOx (right column) hydrogel spheres implanted subcutaneously in mice stained for H&E, Picro-

Sirius red (PSR; collagen displayed as red) and Masson's trichrome (MT; collagen displayed as blue) as well as immunohistochemical (IHC) staining for α-SMA (smooth muscle layer within arterioles displayed as brown stain (indicated by red arrows)). The * denotes the locations of the hydrogel spheres which were lost during processing. The material-tissue interface showing a thin layer of cells is indicated by the black arrow. Scale bar = 20 µm.

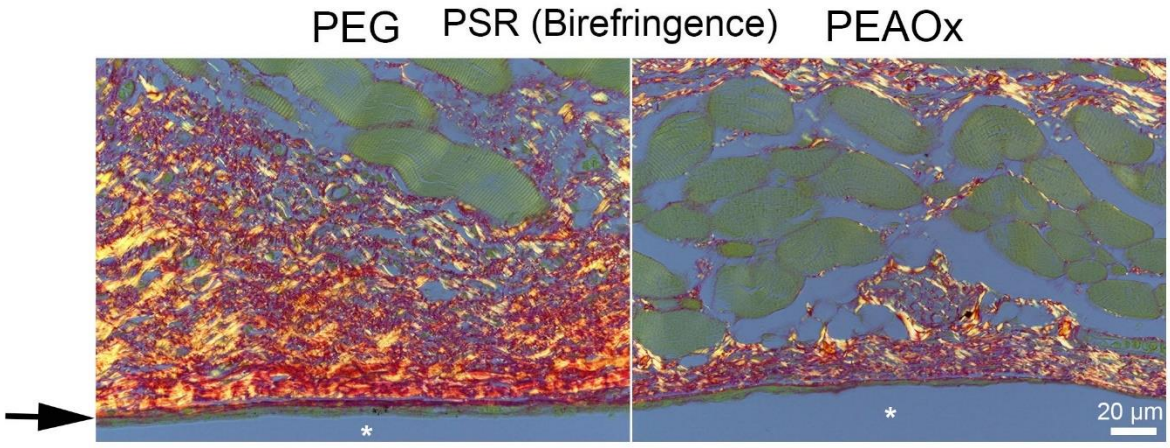

Figure 8: High power views of representative Picro-Sirius Red stained sections under polarized light of explanted PEG and PEAOx spheres. The * denotes the locations of the hydrogel spheres which were lost during processing. The black arrow indicates the material-tissue interface.

Quantification of the histological sections was challenging due to the differences in implantation depth and general heterogeneities in the tissue samples. However, for the PEAOx hydrogels the FBR response appears to be equal to, or slightly improved compared to the PEG hydrogels based on qualitative observations in blind assessments; yet it is acknowledged that caution must be exercised as the apparent difference in connective tissue layer thickness displayed was not a consistent observation and is thus considered to be simply due to variations in the implantation depth.

It has previously been highlighted that it is difficult to predict FBR responses of materials based on their physical-chemical properties alone,[49] however since non-specific protein adsorption is the first stage in

the FBR cascade it is reasonable that for two non-fouling hydrophilic materials such as PEAOx and PEG with similar dimensions that the FBR would be similar but mild. The PEAOx used here was not optimized for non-fouling properties in terms of architecture and hydrophilicity of the monomers. Based on findings by others that certain poly(2-oxazoline)s have been shown to suppress protein adsorption to levels greater than PEG[50] there is great potential to optimize implantable poly(2-oxazoline) hydrogels towards materials with minimal FBR. Predictions alone should, however, not be relied on, not just for the reasons given above, but also because crosslinking of poly(2-oxazoline)s or PEG will lower their degrees of freedom, potentially compromising their protein repelling ability. This study is the first to report the FBR of a poly(2-oxazoline) hydrogel and highlights their potential for implantable materials with minimal host response from this class of polymers.

Conclusions

A novel, highly water-soluble poly(2-oxazoline) polymer containing allyl groups in the side-chains was successfully prepared by amidation of a copolymer of EtOx and C_3MestOx with allyl amine. This copolymer was subsequently used to synthesise hydrogels *via* thiol-ene coupling. The crosslinking was shown to occur very rapidly using UV irradiation with improved kinetics compared with previously reported poly(2-oxazoline) hydrogels,[3] giving them potential for biomedical applications. The faster gelation is ascribed to the potential higher exposure of the allyl groups due to the rather long, hydrophilic amidopropyl spacer. To investigate the biocompatibility of the new hydrogels they were fabricated into hydrogel spheres and used in a side-by-side experiment with PEG hydrogel spheres to examine the foreign body response in a murine sub-dermal implant model. The foreign body response to both materials was similarly minimal and paves the way for future hydrogel implant experiments involving optimized materials for minimal host response, cell and drug delivery.

Acknowledgements

This project was performed with the approval of QUT's Animal Research Ethics Committee (Project approval number: 1900000716). T.D. is supported by the ARC Future Fellowship scheme

(FT150100408). This work was enabled by use of the Central Analytical Research Facility hosted by the Institute for Future Environments at QUT. The authors acknowledge the assistance of Auvro Mridha (University of Sydney) with performing the toxicity tests and Justin Large and Emily Goy (Translational Research Institute, Brisbane) and Flávia Medeiros Savi (QUT) for assistance with histology.

Conflict of interest statement

RH is listed as inventor on patent WO2013103297A1 that covers the amidated PAOx materials reported in this work. JVG and RH are also listed as inventors on patent WO2019224356A1 that covers the amidated PMA materials. TD and RH are listed as inventors on a patent application that covers allylamidated PAOx hydrogels. RH is one of the founders of Avroxa BVBA that commercializes poly(2-oxazoline)s as Ultroxa®. The other authors have no conflicts to declare.

Data availability statement

The raw/processed data required to reproduce these findings cannot be shared at this time as the data also forms part of an ongoing study.

References

1 Li, J. & Mooney, D. J. Designing hydrogels for controlled drug delivery. *Nature Reviews Materials* **1**, doi:10.1038/natrevmats.2016.71 (2016).

2 Annabi, N. *et al.* 25th anniversary article: Rational design and applications of hydrogels in regenerative medicine. *Advanced Materials* **26**, 85-124, doi:10.1002/adma.201303233 (2014).

3 Dargaville, T. R., Lava, K., Verbraeken, B. & Hoogenboom, R. Unexpected Switching of the Photogelation Chemistry When Cross-Linking Poly(2-oxazoline) Copolymers. *Macromolecules* **49**, 4774-4783, doi:10.1021/acs.macromol.6b00167 (2016).

4 Farrugia, B. L., Kempe, K., Schubert, U. S., Hoogenboom, R. & Dargaville, T. R. Poly(2-oxazoline) Hydrogels for Controlled Fibroblast Attachment. *Biomacromolecules* **14**, 2724-2732, doi:10.1021/bm400518h (2013).

5 Hoogenboom, R. Poly(2-oxazoline)s: A polymer class with numerous potential applications. *Angewandte Chemie - International Edition* **48**, 7978-7994, doi:10.1002/anie.200901607 (2009).

6 Dargaville, T. R., Park, J. R. & Hoogenboom, R. Poly(2-oxazoline) Hydrogels: State-of-the-Art and Emerging Applications. *Macromolecular Bioscience* **18**, doi:10.1002/mabi.201800070 (2018).

7 Kelly, A. M. & Wiesbrock, F. Strategies for the Synthesis of Poly(2-Oxazoline)-Based Hydrogels. *Macromol. Rapid Commun.* **33**, 1632-1647, doi:10.1002/marc.201200333 (2012).

8 Hartlieb, M., Schubert, S., Kempe, K., Windhab, N. & Schubert, U. S. Stabilization of Factor VIII by Poly(2-oxazoline) Hydrogels. *J. Polym. Sci., Part A: Polym. Chem.* **53**, 10-14, doi:10.1002/pola.27457 (2015).

9 Ceglowski, M. & Hoogenboom, R. Molecularly Imprinted Poly(2-oxazoline) Based on Cross-Linking by Direct Amidation of Methyl Ester Side Chains. *Macromolecules* **51**, 6468-6475, doi:10.1021/acs.macromol.8b01068 (2018).
10 Hartlieb, M. *et al.* Matrix Supported Poly(2-oxazoline)-Based Hydrogels for DNA Catch and Release. *Biomacromolecules* **15**, 1970-1978, doi:10.1021/bm500236y (2014).
11 Trachsel, L., Broguiere, N., Rosenboom, J. G., Zenobi-Wong, M. & Benetti, E. M. Enzymatically crosslinked poly(2-alkyl-2-oxazoline) networks for 3D cell culture. *Journal of Materials Chemistry B* **6**, 7568-7572, doi:10.1039/c8tb02382d (2018).
12 Trachsel, L., Johnbosco, C., Lang, T., Benetti, E. M. & Zenobi-Wong, M. Double-Network Hydrogels including Enzymatically Crosslinked Poly-(2-alkyl-2-oxazoline)s for 3D Bioprinting of Cartilage-Engineering Constructs. *Biomacromolecules* **20**, 4502-4511, doi:10.1021/acs.biomac.9b01266 (2019).
13 Kalaoglu-Altan, O. I. *et al.* Multireactive Poly(2-oxazoline) Nanofibers through Electrospinning with Crosslinking on the Fly. *ACS Macro Lett.* **5**, 676-681, doi:10.1021/acsmacrolett.6b00188 (2016).
14 Dargaville, T. R. *et al.* Poly(2-oxazoline) Hydrogel Monoliths via Thiol-ene Coupling. *Macromol. Rapid Commun.* **33**, 1695-1700, doi:10.1002/marc.201200249 (2012).
15 Glassner, M., Vergaelen, M. & Hoogenboom, R. Poly(2-oxazoline)s: A comprehensive overview of polymer structures and their physical properties. *Polymer International* **67**, 32-45, doi:10.1002/pi.5457 (2018).
16 Moreadith, R. W. *et al.* Clinical development of a poly(2-oxazoline) (POZ) polymer therapeutic for the treatment of Parkinson's disease – Proof of concept of POZ as a versatile polymer platform for drug development in multiple therapeutic indications. *Eur. Polym. J.* **88**, 524-552, doi:10.1016/j.eurpolymj.2016.09.052 (2017).
17 Olanow, C. W., Standaert, D. G., Kieburtz, K., Viegas, T. X. & Moreadith, R. Once-Weekly Subcutaneous Delivery of Polymer-Linked Rotigotine (SER-214) Provides Continuous Plasma Levels in Parkinson's Disease Patients. *Movement Disorders* **35**, 1055-1061, doi:https://doi.org/10.1002/mds.28027 (2020).
18 Boerman, M. A. *et al.* Next Generation Hemostatic Materials Based on NHS-Ester Functionalized Poly(2-oxazoline)s. *Biomacromolecules* **18**, 2529-2538, doi:10.1021/acs.biomac.7b00683 (2017).
19 Wang, X. *et al.* Thermosensitive Hydrogel Based on Poly(2-Ethyl-2-Oxazoline)–Poly(D,L-Lactide)–Poly(2-Ethyl-2-Oxazoline) for Sustained Salmon Calcitonin Delivery. *AAPS PharmSciTech* **21**, doi:10.1208/s12249-020-1619-1 (2020).
20 You, Y. *et al.* Engineered cell-degradable poly(2-alkyl-2-oxazoline) hydrogel for epicardial placement of mesenchymal stem cells for myocardial repair. *Biomaterials*, 120356, doi:https://doi.org/10.1016/j.biomaterials.2020.120356 (2020).
21 Lorson, T. *et al.* Poly(2-oxazoline)s based biomaterials: A comprehensive and critical update. *Biomaterials* **178**, 204-280, doi:10.1016/j.biomaterials.2018.05.022 (2018).
22 Vegas, A. J. *et al.* Combinatorial hydrogel library enables identification of materials that mitigate the foreign body response in primates. *Nature Biotechnology* **34**, 345-352, doi:10.1038/nbt.3462 (2016).
23 Grainger, D. W. All charged up about implanted biomaterials. *Nature Biotechnology* **31**, 507-509, doi:10.1038/nbt.2600 (2013).
24 Williams, D. F. On the mechanisms of biocompatibility. *Biomaterials* **29**, 2941-2953, doi:10.1016/j.biomaterials.2008.04.023 (2008).
25 Harding, J. L. & Reynolds, M. M. Combating medical device fouling. *Trends in Biotechnology* **32**, 140-146, doi:10.1016/j.tibtech.2013.12.004 (2014).
26 Sehlinger, A., Verbraeken, B., Meier, M. A. R. & Hoogenboom, R. Versatile side chain modification via isocyanide-based multicomponent reactions: Tuning the LCST of poly(2-oxazoline)s. *Polymer Chemistry* **6**, 3828-3836, doi:10.1039/c5py00392j (2015).

27 Bouten, P. J. M., Lava, K., Van Hest, J. C. M. & Hoogenboom, R. Thermal properties of methyl ester-containing poly(2-oxazoline)s. *Polymers* **7**, 1998-2008, doi:10.3390/polym7101494 (2015).
28 Bouten, P. J. M. *et al.* Accelerated living cationic ring-opening polymerization of a methyl ester functionalized 2-oxazoline monomer. *Polymer Chemistry* **6**, 514-518, doi:10.1039/c4py01373e (2015).
29 Mees, M. A. & Hoogenboom, R. Functional Poly(2-oxazoline)s by Direct Amidation of Methyl Ester Side Chains. *Macromolecules* **48**, 3531-3538, doi:10.1021/acs.macromol.5b00290 (2015).
30 Bouten, P. J. M. *et al.* Synthesis of poly(2-oxazoline)s with side chain methyl ester functionalities: Detailed understanding of living copolymerization behavior of methyl ester containing monomers with 2-alkyl-2-oxazolines. *Journal of Polymer Science Part a-Polymer Chemistry* **53**, 2649-2661, doi:10.1002/pola.27733 (2015).
31 Monnery, B. D. *et al.* Defined High Molar Mass Poly(2-Oxazoline)s. *Angewandte Chemie - International Edition* **57**, 15400-15404, doi:10.1002/anie.201807796 (2018).
32 Patent Method for the preparation of uniform, high molar mass cyclic imino ether polymers. (2015).
33 *https://www.nhmrc.gov.au/about-us/publications/australian-code-care-and-use-animals-scientific-purposes (accessed 19 Oct 2020)*.
34 Van Guyse, J. F. R. *et al.* Amidation of methyl ester side chain bearing poly(2-oxazoline)s with tyramine: A quest for a selective and quantitative approach. *Polymer Chemistry* **10**, 954-962, doi:10.1039/c9py00014c (2019).
35 Van Guyse, J. F. R. *et al.* Full and Partial Amidation of Poly(methyl acrylate) as Basis for Functional Polyacrylamide (Co)Polymers. *Macromolecules* **52**, 5102-5109, doi:10.1021/acs.macromol.9b00399 (2019).
36 Kempe, K. *et al.* Multifunctional Poly(2-oxazoline) Nanoparticles for Biological Applications. *Macromol. Rapid Commun.* **31**, 1869-1873, doi:10.1002/marc.201000283 (2010).
37 Viegas, T. X. *et al.* Polyoxazoline: Chemistry, properties, and applications in drug delivery. *Bioconjugate Chem.* **22**, 976-986, doi:10.1021/bc200049d (2011).
38 Platen, M. *et al.* Poly(2-oxazoline)-Based Microgel Particles for Neuronal Cell Culture. *Biomacromolecules* **16**, 1516-1524, doi:10.1021/bm501879h (2015).
39 Luck, S. *et al.* Tailored and biodegradable poly(2-oxazoline) microbeads as 3D matrices for stem cell culture in regenerative therapies. *Biomaterials* **79**, 1-14, doi:10.1016/j.biomaterials.2015.11.045 (2016).
40 Lutolf, M. P. & Hubbell, J. A. Synthesis and physicochemical characterization of end-linked poly(ethylene glycol)-co-peptide hydrogels formed by Michael-type addition. *Biomacromolecules* **4**, 713-722, doi:10.1021/bm025744e (2003).
41 Wang, S., Dalton, P. D. & Dargaville, T. R. Spatial Patterning of Hydrogels via 3D Covalent Transfer Stamping from a Fugitive Ink. *Macromolecular Rapid Communications* **39**, doi:10.1002/marc.201700564 (2018).
42 Anderson, J. M., Rodriguez, A. & Chang, D. T. Foreign body reaction to biomaterials. *Semin. Immunol.* **20**, 86-100, doi:10.1016/j.smim.2007.11.004 (2008).
43 Lynn, A. D., Kyriakides, T. R. & Bryant, S. J. Characterization of the in vitro macrophage response and in vivo host response to poly(ethylene glycol)-based hydrogels. *J. Biomed. Mater. Res., Part A* **93**, 941-953, doi:10.1002/jbm.a.32595 (2010).
44 Van Kuringen, H. P. C. *et al.* Partial Hydrolysis of Poly(2-ethyl-2-oxazoline) and Potential Implications for Biomedical Applications? *Macromolecular Bioscience* **12**, 1114-1123, doi:10.1002/mabi.201200080 (2012).
45 Ulbricht, J., Jordan, R. & Luxenhofer, R. On the biodegradability of polyethylene glycol, polypeptoids and poly(2-oxazoline)s. *Biomaterials* **35**, 4848-4861, doi:10.1016/j.biomaterials.2014.02.029 (2014).

46 Zhang, L. *et al.* Zwitterionic hydrogels implanted in mice resist the foreign-body reaction. *Nature Biotechnology* **31**, 553-+, doi:10.1038/nbt.2580 (2013).
47 Garg, K., Pullen, N. A., Oskeritzian, C. A., Ryan, J. J. & Bowlin, G. L. Macrophage functional polarization (M1/M2) in response to varying fiber and pore dimensions of electrospun scaffolds. *Biomaterials* **34**, 4439-4451, doi:10.1016/j.biomaterials.2013.02.065 (2013).
48 Lattouf, R. *et al.* Picrosirius Red Staining: A Useful Tool to Appraise Collagen Networks in Normal and Pathological Tissues. *Journal of Histochemistry & Cytochemistry* **62**, 751-758, doi:10.1369/0022155414545787 (2014).
49 Klopfleisch, R. & Jung, F. The pathology of the foreign body reaction against biomaterials. *Journal of Biomedical Materials Research Part A* **105**, 927-940, doi:10.1002/jbm.a.35958 (2017).
50 Trachsel, L., Romio, M., Ramakrishna, S. N. & Benetti, E. M. Fabrication of Biopassive Surfaces Using Poly(2-alkyl-2-oxazoline)s: Recent Progresses and Applications. *Adv. Mater. Interfaces*, 9, doi:10.1002/admi.202000943.
51 Byrne, J. P., Blasco, S., Aletti, A. B., Hessman, G. & Gunnlaugsson, T. Formation of Self-Templated 2,6-Bis(1,2,3-triazol-4-yl)pyridine [2]Catenanes by Triazolyl Hydrogen Bonding: Selective Anion Hosts for Phosphate. *Angewandte Chemie International Edition* **55**, 8938-8943, doi:10.1002/anie.201603213 (2016).

Supporting Information

Poly(2-allylamidopropyl-2-oxazoline) based hydrogels: from accelerated gelation kinetics to *in vivo* compatibility in a murine sub-dermal implant model

Tim R. Dargaville, Damien G. Harkin, Jong-Ryul Park, Amanda Cavalcanti, Eleonore C.L. Bolle, Flavia Medeiros Savi, Brooke L. Farrugia, Bryn Monnery, Yann Bernhard, Joachim F. R. Van Guyse, Annelore Podevyn, Richard Hoogenboom

Materials: triazabicyclodecene (TBD, 98%, TCI), ethanolamine (99%, TCI), allylamine (99%, Sigma-Aldrich), *DL*-Dithiothreitol (DTT) (≥ 98%, Sigam-Aldrich), Dowex® 50W X8 Hydrogen form strongly Acidic 50-100 Mesh (Sigma-Aldrich), acetone (>99 % Sigma-Aldrich). Irgacure® 2959 was kindly donated by BASF. polymethyl acrylate (PMA) was purchased from Scientific Polymer Products (40.08% solution in toluene, approx. Mw: 40,000 $g.mol^{-1}$; toluene was removed before use) 4-pentenylamine was synthetized according to a published method.[51]

Synthesis of hydroxyethylacrylamide with allylacrylamide and pentenylacrylamide: The copolymers of hydroxethylacrylamide with allylacrylamide and pentenylacrylamide (Figure 4) were prepared by co-amidation of commercially available PMA, using an excess of amines (mixture of ethanolamine with allylamine or pentenylamine) and in presence of TBD as catalyst, according to the following procedure. PMA (0.5 g, 40 kDa, 0.0125 mmol corresponding to approx. 5.81 mmol of methyl ester group) was weighed in 5 mL flasks (5 mL microwaves tubes). Appropriate amounts of amines (for a total of 6 eq. of amine per methyl ester group) with predetermined ratio (molar ratio 1:1 or 2:1) were introduced in the flasks and the solutions were cooled to 0°C and degassed by argon bubbling for 10 min.

Flask 1A, molar ratio 2:1, ethanolamine (23.25 mmol, 1.39 mL) / allylamine (11.6 mmol, 1.03 mL)

Flask 2A, molar ratio 1:1, ethanolamine (17.43 mmol, 1.04 mL) / allylamine (17.43 mmol, 1.54 mL)

Flask 1B, molar ratio 2:1, ethanolamine (23.25 mmol, 1.39 mL) / 4-pentenylamine (11.6 mmol, 1.16 g)

Flask 2B, molar ratio 1:1, ethanolamine (17.43 mmol, 1.04 mL) / 4-pentenylamine (17.43 mmol, 1.75 g)

TBD (81 mg, 0.58 mmol, 0.1 eq. per methyl ester) was then added to the mixtures and the flasks were flushed with Argon, capped and heated at 80°C over a period of 24h. After return to room temperature, the mixtures were poured into 30 mL of cold acetone to precipitate the polymers. The solutions were centrifuged, and the liquid supernatant discarded. The polymers were further precipitated three times by dissolving in a minimal amount of methanol (2-3 mL) and pouring in cold acetone (30 mL). To remove TBD and residual traces of amines, the resultant polymers were dissolved in water, and for each sample, Dowex (160 mg, twice the mass of TBD) was added. After stirring for 5 hours and filtration to remove the Dowex, water was removed by freeze drying and the resultant solids were dried in a vacuum oven at 40°C overnight to yield the desired pure polymers as white powders.

The polymers were analyzed by FTIR spectroscopy to confirm the full conversion of the methyl ester (at 1726 cm^{-1}) and the observation of the peak of the amide (at 2642 cm^{-1}).

Polymer 1A: ^{1}H NMR (300 MHz, 298 K, D2O) δ(ppm) 1.35-1.85 (m, 2H); 1.90-2.35 (m, 2H); 3.10-3.50 (m, 2H); 3.55-3.75 (m, 2H); 5.15-5.25 (m, 0.07H); 5.75-5.95 (m, 0.03H). The resulting polymer contains 3 mol% allylacrylamide units. The deviation between the theoretical amount of allylacrylamide units based on stoichiometry and the incorporated amount is currently being investigated and will be the focus of a future publication.

Polymer 2A: ^{1}H NMR (300 MHz, 298 K, D2O) δ(ppm) 1.35-1.85 (m, 2H); 1.90-2.35 (m, 2H); 3.10-3.50 (m, 2H); 3.55-3.75 (m, 2H); 5.15-5.25 (m, 0.2H); 5.75-5.95 (m, 0.10H). The resulting polymer contains 10 mol% allylacrylamide units.

Polymer 1B: ^{1}H NMR (300 MHz, 298 K, D2O) δ(ppm) 1.35-1.85 (m, 2H); 1.90-2.35 (m, 2H); 1.90-3.75 (m, 0.12H); 3.10-3.50 (m, 2H); 3.55-3.75 (m, 2H); 5.15-5.25 (m, 0.07H); 5.75-5.95 (m, 0.03H). The resulting polymer contains 3 mol% pentenylacrylamide units.

Polymer 2B: ^{1}H NMR (300 MHz, 298 K, D2O) δ(ppm) 1.35-1.85 (m, 2H); 1.90-2.35 (m, 2H); 1.90-3.75 (m, 0.4H); 3.10-3.50 (m, 2H); 3.55-3.75 (m, 2H); 5.15-5.25 (m, 0.2H); 5.75-5.95 (m, 0.1H). The resulting polymer contains 10 mol% pentenylacrylamide units.

The polymers were analysed by SEC to confirm the mass and dispersity. Starting PMA: Mn = 19.2 kg/mol, Đ = 2.9; Polymer 1A: Mn = 14.4 kg/mol, Đ = 3.6; Polymer 2A: Mn = 36.4 kg/mol, Đ = 3.9 Polymer 1B: Mn = 24.1 kg/mol, Đ = 2.31; Polymer 2B: Mn = 32.9 kg/mol, Đ = 2.28

Curing experiments: Gelation kinetics were studied by performing small strain oscillatory shear experiments on an Anton Paar MCR302 Rheometer with 25 mm parallel plate-plate geometry at room temperature (Figure S3). *In situ* photo-crosslinking experiments were conducted with 10 wt% solutions of polymers in water as the solvent, containing 0.5 equivalent of DTT per double bond (allyl, pentenyl groups), and a concentration of photo-initiator (Irgacure2959) of 10 mol% per DTT. The solution was deposited on the rheometer glass plate and the gap was fixed at 0.4 mm. The storage and loss moduli were measured over a total period over 665 sec with a gamma amplitude for the (oscillating) shear deformation at 0.1 % and a deformation frequency of 1 Hz. The baseline was measured during 1 min, then the samples were irradiated using an Omnicure Series 2000 ultraviolet light source with 365 nm filter and a fibre optic probe fitted under the quartz bottom plate of the rheometer.

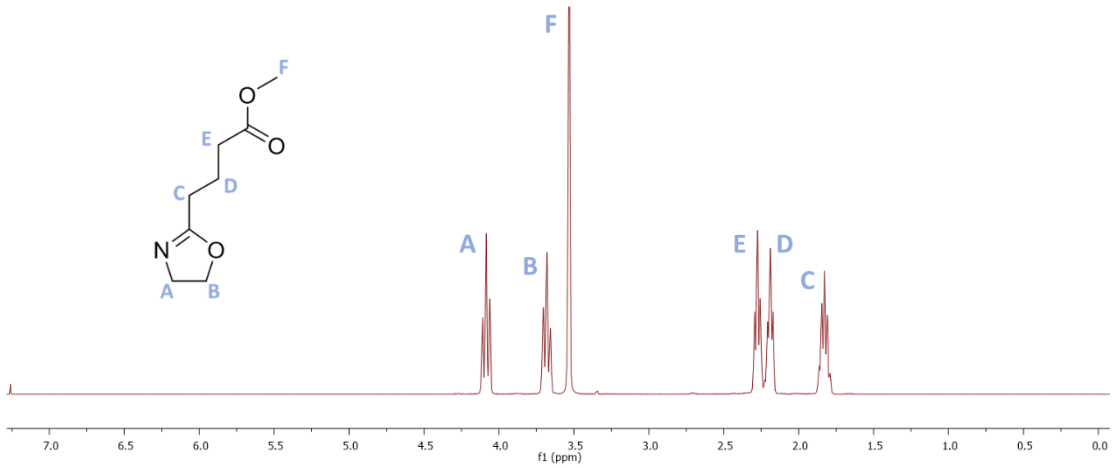

Figure S1: ^{1}H NMR spectrum of the C_3MestOx monomer and peak assignments. The solvent was $CDCl_3$.

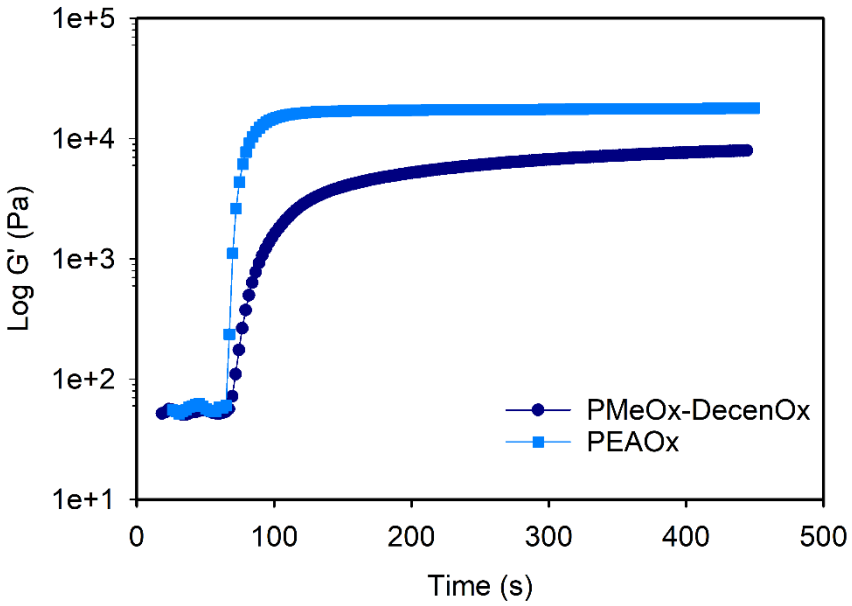

Figure S2: Photo-curing of PEAOx compared with PMeOx-DecenOx. Synthesis of PMeOx-DecenOx has been previously reported.[14]

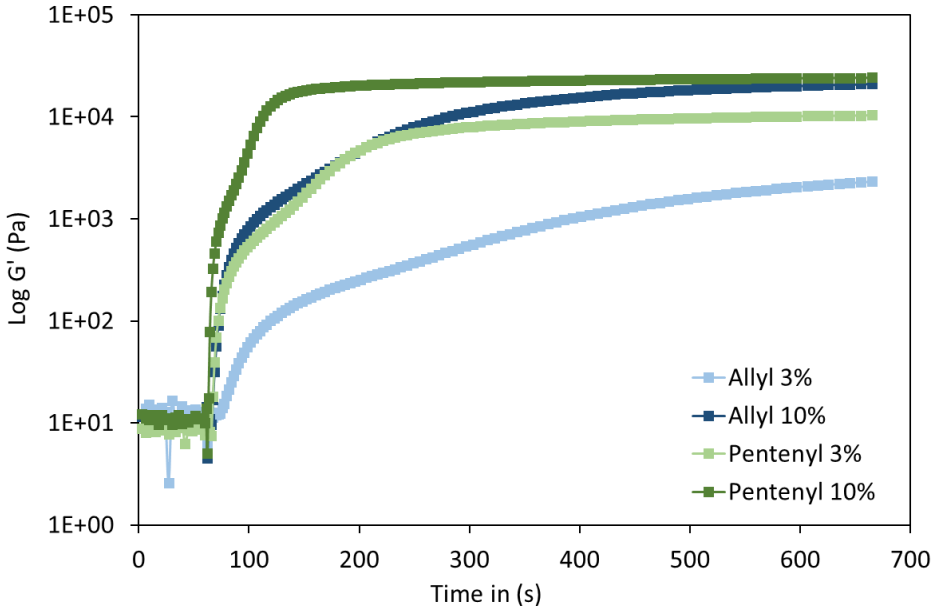

Figure S3: Comparative photo-curing curves of polymers composed of hydroxyethylacrylamide with allylacrylamide or pentenylacrylamide

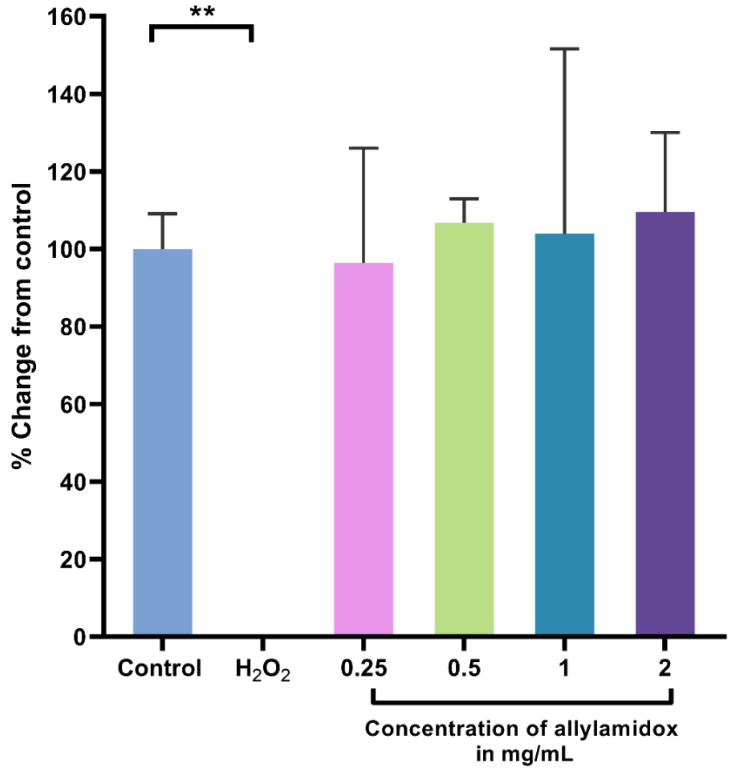

Figure S4: The effects of PEAOx on cell viability (as determined by reduction of the tetrazolium salt, MTS, to coloured formazan product) after 6 hours treatment. Human foetal fibroblasts were used as the test model. Control = no treatment (i.e. negative control), H_2O_2 = positive control for toxicity, 0.25 – 2 mg/mL of PEAOx. Statistical significance was determined by one-way ANOVA and Tukey's multiple comparisons test and accepted were *$p < 0.05$.

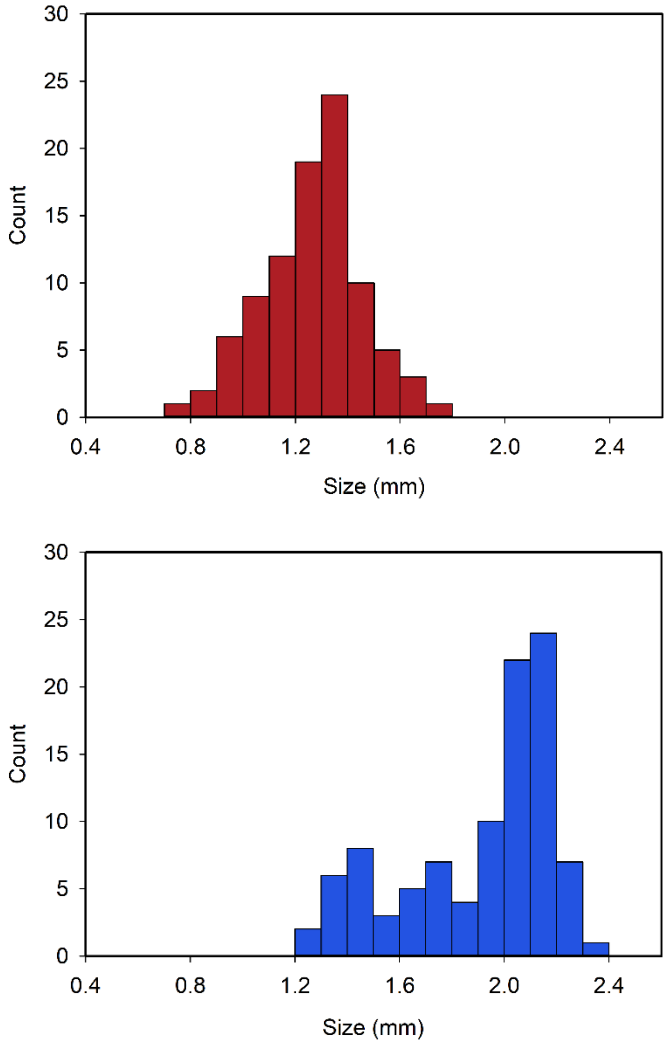

Figure S5: size distribution of PEAOx spheres (top) and PEG spheres (bottom)

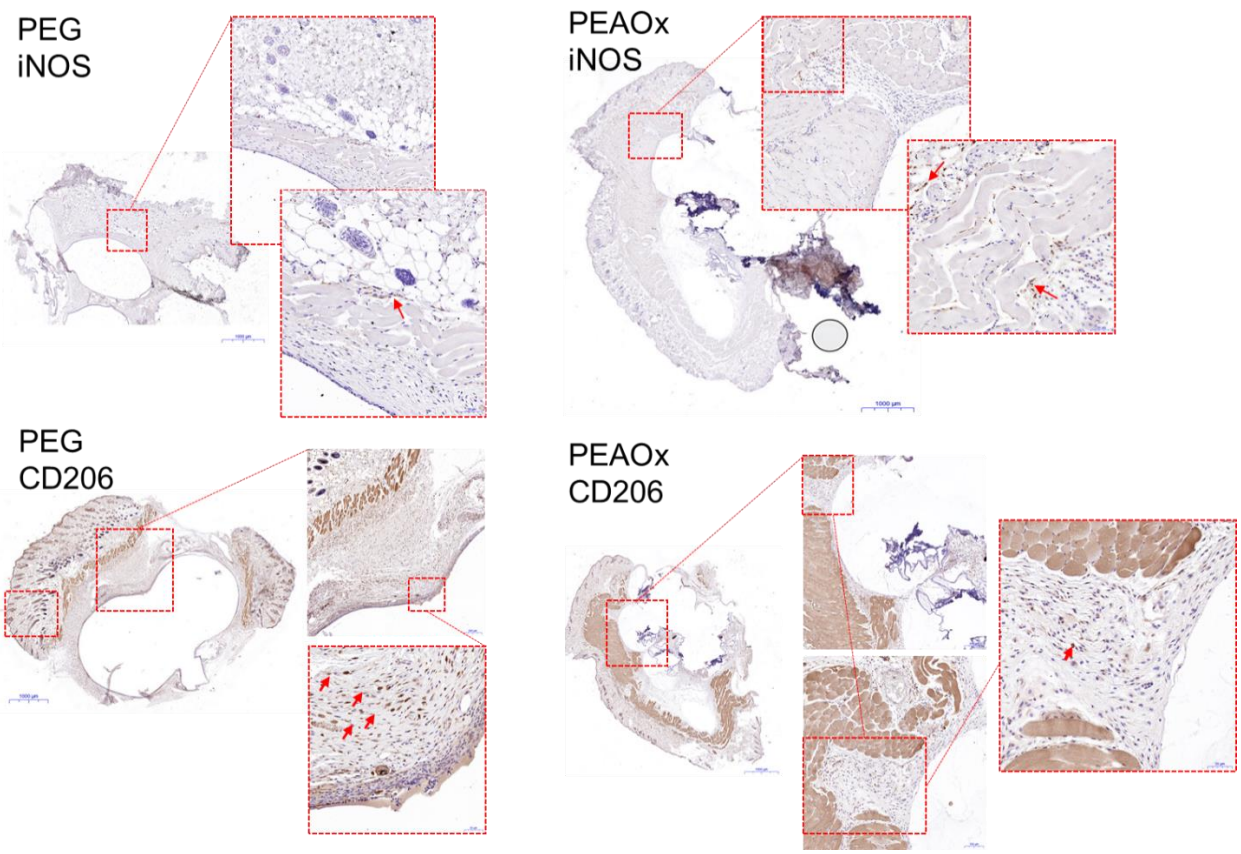

Figure S6: iNOS and CD206 as markers for pro-inflammatory and reparative macrophage phenotypes. Arrows indicate presence of positively stained macrophages. The iNOS antibody (abcam, cat # ab15323) was added in a dilution of 1:200 following antigen retrieval in EDTA buffer for 5 minutes at 95 °C and blocking in 2% BSA for 30 minutes. Sections were incubated with the primary antibody for 1 hour and countered stained with DAB and hematoxylin for 2 minutes. The CD206 mannose receptor (abcam, cat # ab64693) was added in a dilution of 1:100 following antigen retrieval using the same conditions as for iNOS, except the secondary antibody incubation time was 20 seconds.

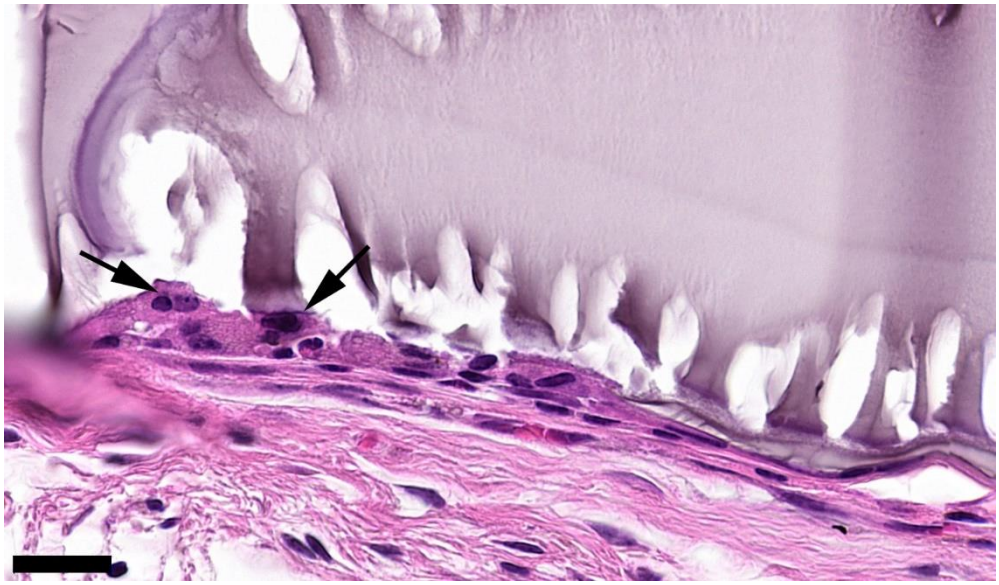

Figure S7: High power views of a typical histological section stained with H&E indicating multi-nucleated giant cells (black arrows) adjacent to the partially intact hydrogel sphere (stained purple). This example is a PEAOx hydrogel sphere implanted subcutaneously. Scale bar = 20 µm.